

Explainable Attention for Few-shot Learning and Beyond

Bahareh Nikpour^{1,2}, Narges Armanfard^{1,2}

¹Department of Electrical and Computer Engineering, McGill University

²Mila - Quebec AI Institute, Montreal, QC, Canada

bahareh.nikpour@mail.mcgill.ca, narges.armanfard@mcgill.ca

Abstract

Attention mechanisms have exhibited promising potential in enhancing learning models by identifying salient portions of input data. This is particularly valuable in scenarios where limited training samples are accessible due to challenges in data collection and labeling. Drawing inspiration from human recognition processes, we posit that an AI baseline’s performance could be more accurate and dependable if it is exposed to essential segments of raw data rather than the entire input dataset, akin to human perception. However, the task of selecting these informative data segments referred to as hard attention finding, presents a formidable challenge. In situations with few training samples, existing studies struggle to locate such informative regions due to the large number of training parameters that cannot be effectively learned from the available limited samples. In this study, we introduce a novel and practical framework for achieving explainable hard attention finding, specifically tailored for few-shot learning scenarios, called FewXAT. Our approach employs deep reinforcement learning to implement the concept of hard attention, directly impacting raw input data and thus rendering the process interpretable for human understanding. Through extensive experimentation across various benchmark datasets, we demonstrate the efficacy of our proposed method.

1. Introduction

Few-shot learning is a challenging field in machine learning, where the goal is to train a model with limited labeled data and generalize its knowledge to new, unseen classes [24]. There are lots of practical applications for few-shot learning methods ranging from computer vision such as image classification [4], activity recognition [10], image retrieval [27], and object tracking [13] to medical applications such as drug discovery [26]. Most of the leading few-shot learning methods are either metric learning-based or meta learner-based [11]. Prototypical Networks (Prot-

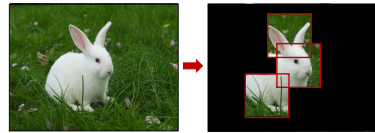


Figure 1. The three attentive regions to define the class rabbit

Net) is one of the most popular metric-based approaches in few-shot learning, proposed by Snell et al. [25]. The main idea behind Prototypical Networks is to learn a metric space where examples from the same class are close to each other, and examples from different classes are far apart. Model-Agnostic Meta-Learning (MAML), is a well-known meta-learning-based method which aims to learn a good initialization that generalizes well across various benchmark datasets and different tasks, allowing the model to adapt efficiently to new tasks during the few-shot learning process [6].

In recent years, attention mechanisms have emerged as a powerful tool for improving computer vision algorithms by enabling models to focus on discriminative regions within the image [12]. That is because not all sections of images possess equal importance, and only certain regions hold valuable information. Attention is particularly inspired by the human visual system which has the ability to focus on specific parts of a scene to rapidly comprehend it. The attention models in the literature mainly fall under two categories: “soft attention”, where different weights show the importance of different data parts, and “hard attention”, where only the important parts of the data are kept and the rest are discarded, allowing for a more interpretable process. Hard attention was first put in place by Minh et al. [14] to reduce computation in convolutional neural networks. Later on, many other techniques were introduced such as [1, 3, 19, 20, 23]. One important benefit of hard attention over soft attention is that it improves computational efficiency by reducing the data size.

Finding hard attention is advantageous in few-shot learning as there are few samples per class and the learning method can be easily misled by noise, background clutter,

and uninformative regions. However, previous studies have encountered difficulties in identifying these informative regions because of the large number of parameters that cannot be learned from the available limited samples. In this paper, we propose a novel, explainable, hard attention-finding approach for few-shot learning, called FewXAT, to detect the attentive areas and enhance performance in few-shot learning. Our method finds hard attention, i.e. informative regions, within an image during the few-shot learning process utilizing deep reinforcement learning. By focusing on the attentive regions, the model can effectively capture the essential cues necessary for accurate classification, even with limited training samples.

The proposed FewXAT framework formulates the problem of finding the attentive regions as a Markov Decision Process (MDP), where a reinforcement learning agent is responsible for finding the optimum locations of multiple attentive areas, called patches, within an image. The agent receives feedback in the form of rewards from the few-shot baseline classifier, guiding it to identify patches that contribute most to the final classification decision. Through this iterative process, the agent becomes adept at identifying informative patches, which facilitates generalization and robustness in scenarios with limited labeled data. Also, keeping only the informative patches and discarding the rest of the information would decrease the memory and computational complexity of the learning model. To enhance the training process, we add an auxiliary task, which is a contrastive learning module, to help finding a better representation of the data.

Deep Reinforcement Learning (RL), has been very successful in several computer vision tasks [15–18, 31]. It has also been used in several research to find hard attention in RGB images for classification tasks such as [2, 5]. Moreover, there are a few methods in the literature aiming at finding soft attention in few-shot learning [22, 30]. There is one method, called reinforced-attention policy (RAP), exploring the idea of finding soft attention using RL in few-shot learning, where attention is found on the feature map of a predefined layer (not the original input image) [7]. As such, RAP is unable to reduce the input image size and requires the entire image for its downstream task. Also, it loses the interpretability of the attentive regions. Unlike RAP, our FewXAT algorithm targets to reduce the required image pixels in the downstream task, i.e. hard attention is found in the original image; hence, one can simply verify the FewXAT outcome by visual inspection of the selected patches that are in line with human attention. Other benefits of hard attention finding on the original image include (but are not limited to) making data coding and transmission more effective and efficient, and allowing the downstream task to be implemented on edge devices which are resource-constrained. To the best of our knowledge, FewXAT is the

first work exploring the idea of finding hard attention for the RGB images in the context of few-shot learning. Moreover, the existing hard attention-finding methods in the classification task have very complex structures, making them impossible to train for a few-shot learning setup.

The contributions of our method are listed below:

- We discovered the novel problem of hard attention finding for RGB images in a few-shot learning setup.
- We proposed a simple framework to address this problem using deep reinforcement learning.
- We added a contrastive learning module as an auxiliary task to enhance the training process.
- We conducted experiments on four popular datasets and got competitive results despite using a small portion of the data, showing the effectiveness of FewXAT.
- By finding hard attention, i.e. attentive regions in the images, we enhanced the contextual understanding and interpretability of the baseline’s predictions.
- By attending to only the informative parts of the image and discarding the rest, our method can decrease the size of the data noticeably which leads to a decrease in the baseline model’s complexity.
- We explored the performance of our proposed method in the classification task, proving the usefulness of our method in other tasks as well.

2. Methodology

In the following, we first begin by introducing the terminology employed in few-shot learning, and then we present our proposed method in detail.

2.1. Problem setting

In few-shot learning, an **episode**¹ refers to a single learning task where a model has to learn from a limited amount of data. The few-shot model learns during many **episode**. Typically, an **episode** consists of two main components: a Support set and a Query set. To train a model, a support set and a query set are randomly selected from the data in each **episode**. This approach of learning is commonly referred to as “ N -way, G -shot” classification, where there are N classes and G samples for each class in the support and query sets. We denote the support set as $SU = \{(x_j, y_j)\}_{j=1}^{N \times G}$, where x_j is the j^{th} sample in the support set and y_j is its corresponding label.

¹Two types of episodes are used in this paper: the episode in the reinforcement learning framework, and the **episode** in the few-shot setup which is defined by bold-sized word to avoid confusion.

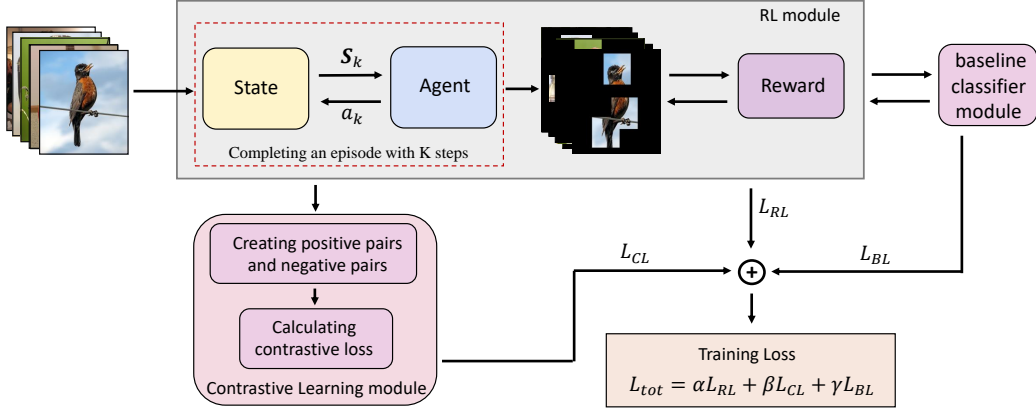


Figure 2. Block diagram of the proposed FewXAT method.

2.2. Proposed method

We assume that every object can be recognized by a number of important regions. Through this paper, we assumed this number to be three, but experiments on different region numbers are presented in section 3.5. Such important regions for recognizing a rabbit are shown in Figure 1. Therefore, FewXAT aims to detect three attentive image patches that can also overlap. As we let the patches overlap, FewXAT can deal with different scales of an object in the images. The size of each patch is fixed and set to $\lfloor 1/3 * d1 \rfloor \times \lfloor 1/3 * d2 \rfloor$ where $\lfloor . \rfloor$ returns the greatest integer less than or equal to its input, and $d1$ and $d2$ refer to the images's width and height, respectively. So, FewXAT keeps maximum 1/3 and minimum 1/9 of the input image. The block diagram of the proposed method is shown in Figure 2. FewXAT consists of three main modules: an RL module, which is responsible for finding the attentive regions, the baseline classifier module, for learning the final classification task, and a contrastive learning module which we add as an auxiliary task to improve the performance and generalization of the model. In short, in the RL module, the state is defined using the data and is fed to the agent. The agent completes an episode of K steps and gets a reward and calculates the loss of the RL module, i.e. L_{RL} . The reward is generated by applying the baseline classifier to the attentive regions of the validation set. The agent's output on the input training data, which includes the three selected patches per image, are given to the baseline classifier to calculate the classifier loss, i.e., L_{BL} . Also, the agent output's on the training data is used to create positive and negative pairs to be used to calculate the contrastive loss, i.e. L_{CL} . At the end, these three losses are added with different weights to generate the total loss, L_{tot} , used to update the networks of all the three modules. The details regarding each module are discussed in the following.

1- RL Module: In our method, we model the process of finding the attentive areas in images as a Markov decision process and solve it with the popular policy-based reinforcement learning algorithm, Monte Carlo policy gradient (REINFORCE) [29]. The agent in its current state takes actions that result in changing its state and receiving a reward. The agent learns to select the important areas in the image, i.e., it finds spatial hard attentions, by maximizing the total expected reward. In this paper the RL agent is run for every image in a batch with size M , and the k^{th} step in the RL episode for the m^{th} sample in the batch is denoted by $\mathcal{T}_{k,m} = (S_{k,m}, A_{k,m}, R_k)$, where $S_{k,m}$, $A_{k,m}$, and R_k are state, action, and reward at the k^{th} step for the m^{th} image in the batch. One single episode is denoted as $\mathcal{T}_m = (S_{1,m}, A_{1,m}, R_1, \dots, S_{K,m}, A_{K,m}, R_K)$. State, agent, action, and reward in the proposed process are as follows:

State: We define the state $S_{k,m}, m = 1, \dots, M$ as the concatenation of the m^{th} original image in the batch, I_m , and the output of the agent with the selected areas in the previous step of the episode, $I_{k-1,m}$, i.e. $S_{k,m} = [I_m, I_{k-1,m}]$. $I_{k-1,m}$ has the same size as the original I_m , where only the selected patches are present in the image and all the remaining parts are set to zero. $I_{k-1,m}$ is shown in the right side of Figure 3. In the initial state $S_{0,m}$, $I_{0,m}$ is initiated such that the patches are located side-by-side at the top of the image as can be seen in Figure 4.

Agent: The agent can be any neural network structure that is capable of dealing with image data. At each step of the episode, i.e. the k^{th} step, and for the m^{th} image, the agent outputs the probability matrix $P_{k,m}$, which will be used to define the actions it should take.

Action: The action defines the direction of move-

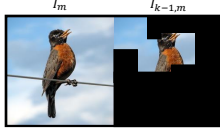


Figure 3. The agent's state $S_{k,m}$, which is concatenation of the original image I_m , and the image output of the agent in the $k-1^{th}$ step of the episode $I_{k-1,m}$, i.e. $S_{k,m} = [I_m, I_{k-1,m}]$

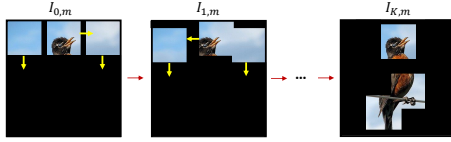


Figure 4. An example of $I_{k,m}$, $\{k = 0, \dots, K\}$ during one episode in our proposed method. The actions, shown in yellow arrows, for step 1 are go down (\downarrow), go right (\rightarrow), and go down (\downarrow) for the first, second, and third regions respectively, which results in $I_{1,m}$. After completing an episode, the agent outputs the regions found in $I_{K,m}$.

ments of the patches. Therefore, for each patch, five actions have been designed: go up, down, left, right, and apply no change. All the movements are done with step size b . For the m^{th} image, each action is denoted by $a_{k,m}^l$ where k refers to the k^{th} step of the RL episode and $l \in \{1, 2, 3\}$ shows the l^{th} attentive region. The actions are sampled from a categorical distribution formed based on the probability output of the agent, $P_{k,m}$. An example of one episode is depicted in Figure 4.

Reward: The reward should reflect how good the action of the agent is in reaching its goal. In our method, the goal is improving or maintaining the baseline's performance while reducing the complexity (and hence improving interpretability). Therefore, the baseline is used to evaluate the output of the agent in step k of the episode. We evaluate the agent's performance at the k^{th} step, by applying it to a random batch of a validation set with $N \times G$ samples for both support and query sets. Using a validation set increases the method's generalization ability. To obtain the reward, first, we let the agent find the three attentive regions in each image of the validation set; then, the three regions are concatenated next to each other, as is shown in Figure 5. Then, it is fed to the baseline in the validation mode to get accuracy. The validation accuracy i.e. Acc_{val}^k is considered as the reward as is defined below:

$$R_k = Acc_{val}^k \quad (1)$$

Training with REINFORCE: The goal of our reinforcement learning agent is learning a policy function (which finds optimum locations of attentive areas) by maximizing

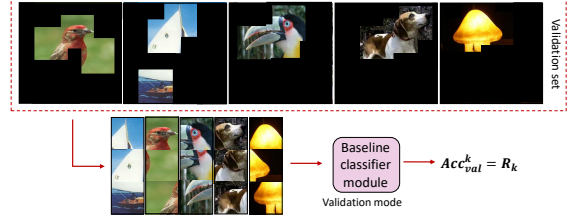


Figure 5. An example of validation batch after finding the attentive region in step k . The new batch of validation samples is given to the baseline, and the output accuracy is considered the reward.

the expected reward $\mathcal{R}(\theta)$ shown below:

$$\mathcal{R}(\theta) = E_{p_\theta(a_{k,m}^l)}[R_k], \quad (2)$$

where $p_\theta(a_{k,m}^l)$ is the probability distribution of the possible actions for the l^{th} patch, and E shows the expectation over l , m and k where $l = \{1, \dots, 3\}$, $k = \{1, \dots, K\}$ and $m = \{1, \dots, M\}$. We utilize REINFORCE, which is a popular policy gradient algorithm [29] to maximize the expected reward and, therefore, find the optimal parameter θ which is a parameter of the function approximating the policy. Following REINFORCE, the gradient of the expected reward in the k^{th} step of the episode, with respect to the parameter θ , is found below:

$$\nabla_\theta \mathcal{R}(\theta) = E_{p_\theta(a_{k,m}^l)}[R_k \nabla_\theta \ln \pi_\theta(a_{k,m}^l | S_{k,m})], \quad (3)$$

where π_θ denotes the policy function, and $S_{k,m}$ is the state of the m^{th} image in the batch at the k^{th} step as $S_{k,m} = [I_m, I_{k-1,m}]$. As was mentioned before, during each episode, the agent takes K steps for each image in the batch. Therefore, we compute the average gradient over M samples in the batch as:

$$\nabla_\theta \mathcal{R}(\theta) \approx \frac{1}{KM} \sum_{k=1}^K \sum_{m=1}^M \sum_{l=1}^3 \nabla_\theta \ln \pi_\theta(a_{k,m}^l | S_{k,m}), \quad (4)$$

where $a_{k,m}^l$ is the action for the l^{th} patch of the m^{th} image in the batch in the k^{th} step of the episode, and $S_{k,m}$ is state of the m^{th} image in the batch.

In order to enhance convergence and decrease variance during the training of θ , we normalize the reward by subtracting a constant baseline value c . This baseline c corresponds to the mean reward across episodes. Hence, the gradient becomes:

$$\nabla_\theta \mathcal{R}(\theta) \approx \frac{1}{KM} \sum_{k=1}^K [(R_k - c) \sum_{m=1}^M \sum_{l=1}^3 \nabla_\theta \ln \pi_\theta(a_{k,m}^l | S_{k,m})], \quad (5)$$

Therefore, the loss of policy to minimize can be shown as:

$$L_{RL} = -\frac{1}{KM} \sum_{k=1}^K [(R_k - c) \sum_{m=1}^M \sum_{l=1}^3 \ln \pi_\theta(a_{k,m}^l | S_{k,m})] \quad (6)$$

2- Training the Baseline model: The baseline is responsible for learning the desired task, which is the classification of the few-shot samples using only the selected patches. We train the baseline during policy training using the train data. To do so, the output attentive regions for each train data, provided by the policy network, are concatenated next to each other (similar to what was done for the validation set when obtaining the reward, shown in Figure 5). More specifically, the concatenation of three selected patches from each training image generates a new image that is three times the size of a single patch. The new images are used as training data for the baseline model. The baseline loss L_{BL} , defined in (7), is calculated on its training data. Note that any few-shot classification method can be used as the FewXAT baseline module. In this paper, we used the ProtoNet algorithm as the baseline, as it is one of the most popular and well-performing learning methods for few-shot learning [25]. For each class, ProtoNet calculates a prototype vector by averaging the embeddings (obtained from a neural network) of the support samples belonging to that class in the feature space. The prototype represents the characteristic features of the class. During training, ProtoNet minimizes the distance between the embedding of a query sample and the prototype of the query sample's true class, while maximizing the distance from the prototypes of other classes. This encourages the model to learn prototypes that can effectively represent classes and differentiate them. The loss of ProtoNet is calculated as follows:

$$L_{BL} = -\log(\text{softmax}(-\|g(x_q), v_y\|)) \quad (7)$$

where $g(x_q)$ is the embedded representation of the query sample, v_y is the prototype representation of the correct class y in the support set SU , $\|\cdot\|$ denotes the distance (e.g., Euclidean) between two vectors, and $\text{softmax}(\cdot)$ computes the softmax function over the negative distance.

3- Contrastive Learning Module: In general, adding auxiliary tasks is advantageous from various perspectives. It can improve the performance of the main task and help to increase the generalization by encouraging the model to learn more general features. Moreover, learning the auxiliary task along with the main task usually helps with faster convergence by providing additional gradients that guide the learning process and can prevent the model from getting stuck in local minima. Lastly, the auxiliary task can force the model to learn meaningful and disentangled representations of the input data, making it easier to extract important features and patterns. Motivated by the mentioned benefits, we added the contrastive learning module as an auxiliary task to help our method's training procedure.

Contrastive learning is a learning technique that aims to learn useful representations by bringing similar data sam-

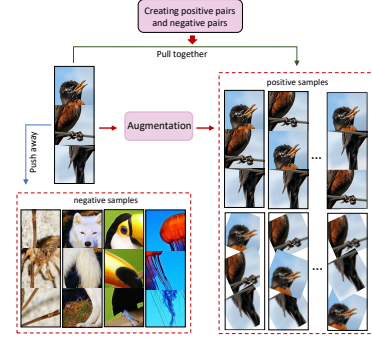


Figure 6. An example of creating positive and negative pairs in 5-way scenario. The first row in positive samples shows every permutation of the attentive regions. The second row shows the rotated attentive regions and their permutation.

ple, i.e. positives, closer to each other in the learned representation space while pushing dissimilar data points, i.e. negatives, farther apart. In our method, we use the support set and query set in the batch to create positive and negative pairs. Pairs from the same class and their augmentation are considered as positive pairs, while negative pairs are pairs from different classes. The augmentations we used for each sample are: (1) every possible permutation of concatenating the three selected attentive regions next to each other, as we do not want our method to be sensitive to the concatenation order of the selected patches; (2) a random rotation in the range -45 degrees and 45 degrees, to make our method robust to rotation. Therefore, we have 12 augmentations, and 12 positive pairs as a result, for each sample, as can be seen in Figure 6. After augmentation and creating positive and negative pairs, the contrastive loss is calculated. As the labels of data samples are available, we use the supervised contrastive loss (SupCon loss) [8] as follows:

$$L_{CL} = \sum_{i \in W} \frac{-1}{|O(i)|} \sum_{o \in O(i)} \log \frac{\exp(f_i \cdot f_o / \tau)}{\sum_{u \in U(i)} \exp(f_i \cdot f_u / \tau)} \quad (8)$$

where $i \in W \equiv \{1, \dots, 2Z\}$, is the index of an arbitrary augmented sample (Z is the number of randomly sampled pairs). $O(i)$ shows the indices of the positive pairs distinct from i , and $|O(i)|$ denotes its cardinality, $U(i) \equiv W \setminus i$, f_ζ shows the output representation of the network for the ζ th index, and τ is the temperature parameter to control the similarity scale. For more details, see [8].

4- Training the algorithm

After the calculation of the three losses, i.e. the policy loss, the baseline loss, and the contrastive learning loss, the total loss to be minimized is calculated as:

$$L_{tot} = \alpha L_{RL} + \beta L_{CL} + \gamma L_{BL} \quad (9)$$

where α , β , and γ are hyperparameters to control the contribution of their corresponding loss term. The pseudo-code of the proposed FewXAT framework is presented in Algorithm 1 in the Appendix. In short, a batch of few-shot tasks is firstly sampled and the train data, including both support set and query set, is given to the agent, K steps are completed, and the reward R_k is calculated in each step k of the method. The output of the agent is the coordinates of the three patches. Using the output of the agent, the new train set including samples with the attentive regions is created, and the loss of baseline is found using this new set. Then, the CL loss is computed using the output embedding of the contrastive learning network on the data and its augmentation. Having the three losses, the total loss is calculated, and all three networks are updated. This process is repeated for a defined number of **episodes** until the three networks are trained.

In the testing phase, the train data is first given to the policy, the selected patches are concatenated, and the baseline is trained on this new train set. Then, the test data is fed to the policy, and the new test data obtained by concatenation of the selected patches is classified using the trained baseline.

3. Experiments

We conducted experiments on four commonly employed datasets for few-shot learning, MiniImageNet [21], CIFAR-FS [9], FC-100 [9], and CUB [28], with ProtoNet [25] as the baseline model. Datasets detail is presented in the Appendix.

3.1. FewXAT for fewshot

In our experiments, ProtoNet was employed with four different structures, namely Conv-4, ResNet-10, ResNet-12, and ResNet-18, and the corresponding accuracy results are detailed in Table 1. The first row of the table showcases the test results of the baselines on the original data. The second row displays baseline testing results after randomly selecting three image patches with a uniform distribution. The last row illustrates the outcomes obtained by the attentive patches selected using FewXAT. If the accuracy after applying FewXAT, denoted as FewXAT(baseline), falls within the range of baseline accuracy ± 0.5 , we assume the performance is maintained. In cases where FewXAT(baseline) performance is 0.5% greater than the baseline accuracy, we infer an improvement compared to the baseline that employs the whole image for classification. As can be observed, FewXAT consistently either improves or maintains performance. This is particularly advantageous because, firstly, downsizing the images through selective patch inclusion reduces complexity. Secondly, retaining essential regions enhances interpretability. Moreover, when comparing FewXAT results with random selection, all outcomes notably outperform, indicating the effectiveness of the pro-

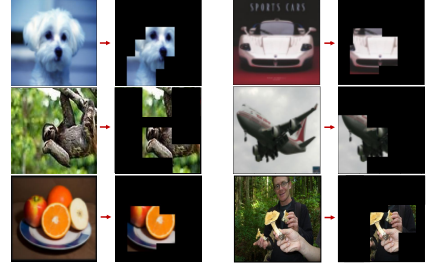


Figure 7. Visualization of the attentive regions found by FewXAT

posed method in identifying informative and discriminative patch locations.

To further demonstrate the remarkable effectiveness of FewXAT, we extend our evaluation to another state-of-the-art few-shot classification method, namely MAML [6], which is a meta-learner-based model. The results, presented in Table 2, reaffirm that FewXAT consistently either improved or maintained accuracy, which highlights the general applicability of FewXAT, demonstrating its capacity to enhance performance regardless of the chosen baseline.

3.2. Visualization of the learned hard attention

FewXAT's selected patches for a few samples are illustrated in Figure 7. The visual output of FewXAT affirms its consistency with human perception, contributing to the interpretability of the learning model. For instance, in the first image, representing the class dog, the attentive regions identified include the eyes and nose of the dog, serving as discriminative features from other classes. Also, retaining less than one-third of the image significantly reduces the data size.

3.3. Effect of Contrastive Learning module

To assess the impact of incorporating the auxiliary task contrastive learning (CL) on performance, we conducted experiments by excluding this module from our method and running it on our datasets using ProtoNet (with ResNet-10). The accuracy results are presented in Table 3. It is evident that integrating the CL module significantly enhances performance, guiding the model to acquire better representations. This improvement is particularly crucial in a few-shot setting where the scarcity of samples often leads to a diminished generalization ability in the classification model. The inclusion of the CL module contributes to the learning of semantically meaningful features, thereby enhancing overall generalization.

3.4. Impact of hyperparameters b and K

As previously discussed, b represents the step size of the agent in the right/left/up/down directions, while K signifies the total number of steps the agent takes during an episode.

Table 1. The accuracy results (in percent) on MiniImageNet, CIFAR-FS, FC-100, and CUB datasets before and after applying FewXAT, and with random selection for 5-shot 5-way (5-s 5-w), and 1-shot 5-way (1-s 5-w) settings.

methods	Dataset	MiniImageNet		CIFAR-FS		FC-100		CUB					
		5-s	5-w	1-s	5-w	5-s	5-w	1-s	5-w	5-s	5-w	1-s	5-w
Conv-4		66.98	48.12	77.98	67.12	48.74	31.47	75.12	50.46				
ResNet-10		71.12	49.98	81.26	70.15	51.72	36.41	83.47	72.12				
ResNet-12		70.98	50.14	82.35	71.30	51.52	38.26	85.72	74.91				
ResNet-18		71.88	50.45	82.92	72.06	52.34	38.22	86.07	75.04				
Random(Conv-4)		48.76	32.11	65.14	49.67	42.12	25.69	68.21	35.12				
Random(ResNet-10)		53.76	36.12	70.06	55.14	45.22	29.88	70.32	37.03				
Random(ResNet-12)		53.44	36.14	73.12	56.14	44.29	23.12	70.14	42.22				
Random(ResNet-18)		54.15	35.12	76.33	53.12	44.85	25.12	68.34	56.12				
FewXAT(Conv-4)		68.32	48.89	78.23	67.94	50.21	31.87	76.11	53.21				
FewXAT(ResNet-10)		73.96	52.72	82.47	69.94	53.28	37.91	83.12	73.79				
FewXAT(ResNet-12)		73.22	51.93	82.51	70.23	53.44	37.5	85.29	74.12				
FewXAT(ResNet-18)		73.24	50.61	82.81	72.024	53.72	38.62	87.31	74.96				

Table 2. The accuracy results (in percent) on MiniImageNet, CIFAR-FS, FC-100, and CUB datasets before and after applying FewXAT, using MAML baseline, for 5-shot 5-way (5-s 5-w), and 1-shot 5-way (1-s 5-w) settings.

methods	Dataset	MiniImageNet		CIFAR-FS		FC-100		CUB					
		5-s	5-w	1-s	5-w	5-s	5-w	1-s	5-w	5-s	5-w	1-s	5-w
Conv-4		63.15	47.2	74.27	65.12	48.35	30.12	75.75	54.73				
ResNet-10		66.12	53.98	78.52	66.24	51.23	33.32	79.93	69.12				
ResNet-12		65.14	52.85	79.11	67.54	51.07	36.41	81.18	68.32				
ResNet-18		67.01	54.69	80.12	68.15	51.12	36.54	82.54	68.15				
FewXAT(Conv-4)		63.62	47.39	74.11	66.51	49.69	33.02	76.21	54.98				
FewXAT(ResNet-10)		69.55	54.22	80.21	66.37	50.97	34.13	83.49	71.22				
FewXAT(ResNet-12)		69.30	53.49	78.92	67.35	51.26	35.72	82.94	71.53				
FewXAT(ResNet-18)		68.93	54.76	80.24	67.87	51.23	36.38	82.59	70.89				

The selection of these hyperparameters is closely inter-linked, with both needing careful consideration to enable the agent to thoroughly explore the entire image. To assess their influence on our method’s performance, FewXAT was applied to miniImagenet using the Protonet(Conv-4) baseline, and we considered the following parameter combinations: $(b, K) : (1, 20), (1, 40), (3, 20), (7, 15)$. The resulting accuracy values (in percent) were 56.98, 68.43, 68.32, and 53.21, respectively, with images sized at 84×84 . As can be seen, setting the step size to 1, despite being very small, and completing 20 steps is insufficient to thoroughly explore the entire image. Doubling K , however, significantly enhances performance. Yet, increasing K has the drawback of slowing down the training process, which is undesirable. Setting b to 7, representing a large step size, leads to an unsatisfactory outcome, causing the agent to leap over crucial and informative regions that might remain undiscovered through the search process. Therefore, a trade-off exists when selecting b and K . The smaller step size positively influences performance but concurrently decelerates policy training. Conversely, setting it too large can disrupt

the search process. Throughout all our experiments, we consistently set b and K to 3 and 20, although optimal performance may be achieved by fine-tuning these values for each dataset individually.

3.5. Changing size of the attentive regions

To show the impact of patch size, we designed an experiment on a 5-s 5-w scenario for the MiniImageNet, where the $d1(d2)$, i.e. the width(height) of the patches, is the rounded number obtained by multiplying the $d1(d2)$ of the original image by a number selected from the set $\{1/12, 3/12, 4/12, 6/12, 8/12\}$. The accuracy results are plotted in Figure 8. As observed, the accuracy is very low when $d1$ and $d2$ are set to the too small value of $1/12$ of the original image’s width and height. The accuracy increases by increasing the patch size; e.g., with $3/12$, we obtained quite accurate results that demonstrate the effectiveness of FewXAT in selecting informative and discriminating regions. However, the accuracy slightly drops when the size reaches $8/12$, which at least covers $2/3$ of the image width (height). This behavior confirms that not all the information in the

Table 3. The accuracy results of FewXAT with and without including the Contrastive Learning module on MiniImageNet, CIFAR-FS, FC-100, and CUB datasets with ProtoNet(ResNet-10) as baseline, for 5-shot 5-way (5-s 5-w), and 1-shot 5-way (1-s 5-w) settings.

Dataset methods	MiniImageNet		CIFAR-FS		FC-100		CUB	
	5-s	5-w	1-s	5-w	5-s	5-w	1-s	5-w
FewXAT with the CL module	73.96	52.72	82.47	69.94	53.28	37.91	83.12	73.79
FewXAT without the CL module	65.22	49.18	79.34	66.82	49.47	35.22	78.34	69.57

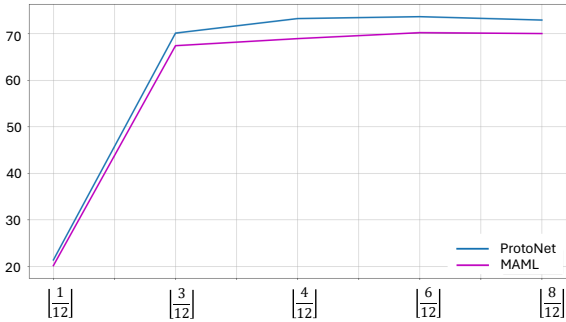


Figure 8. The performance of FewXAT with different patch sizes with the two baselines classifier modules: ProtoNet and MAML.

image is useful and that selecting the informative parts improves performance. It should be mentioned that we observe the best accuracy for the size 6/12 in this plot, but for consistency across the used datasets, we reported all the results for the size 4/12. Note that there is a trade-off between patch size and the data reduction property, which should be taken into consideration depending on the task at hand.

3.6. Run time improvement

The proposed FewXAT method achieves a reduction in data size by retaining a maximum of 1/3 of the image. Consequently, the number of parameters required to train the baseline classifier diminishes, resulting in expedited training and testing. To validate this proposition, we conducted training and testing sessions for the ProtoNet baseline (with Conv-4) on miniImageNet, comparing runs with the original data against runs with only the three attentive regions selected by FewXAT. With FewXAT, the training and testing run times, including the time needed for selecting patches, are 13.43 and 0.18 hours in the 5-s 5-w setting, and 6.01 and 0.11 hours in the 1-s 5-w setting, respectively. In contrast, for the original image, the corresponding times are 21.33 and 0.22 hours in the 5-s 5-w setting, and 12.32 and 0.12 hours in the 1-s 5-w setting, respectively. As anticipated, the selection of attentive areas significantly decreases run time in both the training and testing phases. This reduction is particularly advantageous for resource efficiency and online applications. These experiments were conducted using a Tesla P100-PCIE-16GB GPU.

Table 4. Classification accuracy (in percent) of the two different baseline models with and without FewXAT.

Method	ImageNet10	ImageDog
Conv-4	66.08	53.21
ResNet50	70.23	58.94
FewXAT(Conv-4)	69.27	56.11
FewXAT(ResNet50)	72.18	60.64

3.7. Beyond few-shot learning

To further demonstrate the effectiveness of our proposed method, we applied FewXAT to the regular classification task using two widely recognized benchmark datasets: ImageNet10 and ImageNetdog. These datasets represent subsets of the larger ImageNet dataset. For our baseline models, we opted for Conv-4 and ResNet-50. The accuracy results, both before and after applying FewXAT (i.e., after selecting the attentive patches), are outlined in Table 4. The last row of the table shows our proposed method significantly enhances the performance of the baseline models, concurrently eliminating redundant information and reducing data size. This experiment confirms that the proposed framework not only proves to be beneficial in few-shot learning but also extends its utility to other downstream tasks, including classification and potentially representation learning. Additionally, it provides an interpretable patch selection, enhancing the transparency of the model’s decision-making process.

4. Conclusion

FewXAT stands as a novel Explainable Attention mechanism method crafted to augment its baseline by introducing informative regions. Experimental results substantiate the effectiveness of our approach, revealing performance enhancements or maintenance in few-shot learning tasks, accompanied by a notable reduction in complexity and improved interpretability. Moreover, FewXAT showcases promising results in regular classification tasks, suggesting its potential applicability in a broader spectrum of computer vision tasks.

References

- [1] Bogdan Alexe, Nicolas Heess, Yee Teh, and Vittorio Ferrari. Searching for objects driven by context. *Advances in Neural Information Processing Systems*, 25, 2012.
- [2] Jimmy Ba, Volodymyr Mnih, and Koray Kavukcuoglu. Multiple object recognition with visual attention. *arXiv preprint arXiv:1412.7755*, 2014.
- [3] Jimmy Ba, Russ R Salakhutdinov, Roger B Grosse, and Brendan J Frey. Learning wake-sleep recurrent attention models. *Advances in Neural Information Processing Systems*, 28, 2015.
- [4] Guneet S Dhillon, Pratik Chaudhari, Avinash Ravichandran, and Stefano Soatto. A baseline for few-shot image classification. *arXiv preprint arXiv:1909.02729*, 2019.
- [5] Gamaleldin Elsayed, Simon Kornblith, and Quoc V Le. Saccader: Improving accuracy of hard attention models for vision. *Advances in Neural Information Processing Systems*, 32, 2019.
- [6] Chelsea Finn, Pieter Abbeel, and Sergey Levine. Model-agnostic meta-learning for fast adaptation of deep networks, 2017.
- [7] Jie Hong, Pengfei Fang, Weihao Li, Tong Zhang, Christian Simon, Mehrtash Harandi, and Lars Petersson. Reinforced attention for few-shot learning and beyond, 2021.
- [8] Prannay Khosla, Piotr Teterwak, Chen Wang, Aaron Sarna, Yonglong Tian, Phillip Isola, Aaron Maschinot, Ce Liu, and Dilip Krishnan. Supervised contrastive learning. *Advances in neural information processing systems*, 33:18661–18673, 2020.
- [9] Alex Krizhevsky, Geoffrey Hinton, et al. Learning multiple layers of features from tiny images. 2009.
- [10] Sai Kumar Dwivedi, Vikram Gupta, Rahul Mitra, Shuaib Ahmed, and Arjun Jain. Protagan: Towards few shot learning for action recognition, 2019.
- [11] Zhenguo Li, Fengwei Zhou, Fei Chen, and Hang Li. Metasgd: Learning to learn quickly for few-shot learning. *arXiv preprint arXiv:1707.09835*, 2017.
- [12] Shikun Liu, Edward Johns, and Andrew J Davison. End-to-end multi-task learning with attention. In *Proceedings of the IEEE/CVF conference on computer vision and pattern recognition*, pages 1871–1880, 2019.
- [13] Anay Majee, Kshitij Agrawal, and Anbumani Subramanian. Few-shot learning for road object detection. In *AAAI Workshop on Meta-Learning and MetaDL Challenge*, pages 115–126. PMLR, 2021.
- [14] Volodymyr Mnih, Nicolas Heess, Alex Graves, et al. Recurrent models of visual attention. *Advances in neural information processing systems*, 27, 2014.
- [15] Volodymyr Mnih, Koray Kavukcuoglu, David Silver, Alex Graves, Ioannis Antonoglou, Daan Wierstra, and Martin Riedmiller. Playing atari with deep reinforcement learning. *arXiv preprint arXiv:1312.5602*, 2013.
- [16] Bahareh Nikpour and Narges Armanfard. Joint selection using deep reinforcement learning for skeleton-based activity recognition. In *2021 IEEE International Conference on Systems, Man, and Cybernetics (SMC)*, pages 1056–1061. IEEE, 2021.
- [17] Bahareh Nikpour and Narges Armanfard. Spatial hard attention modeling via deep reinforcement learning for skeleton-based human activity recognition. *IEEE Transactions on Systems, Man, and Cybernetics: Systems*, 2023.
- [18] Bahareh Nikpour, Dimitrios Sinodinos, and Narges Armanfard. Deep reinforcement learning in human activity recognition: A survey. 2024.
- [19] Samrudhdhi B Rangrej and James J Clark. A probabilistic hard attention model for sequentially observed scenes. *arXiv preprint arXiv:2111.07534*, 2021.
- [20] Marc’Aurelio Ranzato. On learning where to look. *arXiv preprint arXiv:1405.5488*, 2014.
- [21] Sachin Ravi and Hugo Larochelle. Optimization as a model for few-shot learning, 2016.
- [22] Mengye Ren, Renjie Liao, Ethan Fetaya, and Richard Zemel. Incremental few-shot learning with attention attractor networks. *Advances in neural information processing systems*, 32, 2019.
- [23] Soroush Seifi, Abhishek Jha, and Tinne Tuytelaars. Glimpse-attend-and-explore: Self-attention for active visual exploration. In *Proceedings of the IEEE/CVF International Conference on Computer Vision*, pages 16137–16146, 2021.
- [24] Guangyuan Shi, Jiaxin Chen, Wenlong Zhang, Li-Ming Zhan, and Xiao-Ming Wu. Overcoming catastrophic forgetting in incremental few-shot learning by finding flat minima. *Advances in neural information processing systems*, 34:6747–6761, 2021.
- [25] Jake Snell, Kevin Swersky, and Richard Zemel. Prototypical networks for few-shot learning. *Advances in neural information processing systems*, 30, 2017.
- [26] Daniel Vella and Jean-Paul Ebejer. Few-shot learning for low-data drug discovery. *Journal of Chemical Information and Modeling*, 63(1):27–42, 2022.
- [27] Yu-Xiong Wang, Liangke Gui, and Martial Hebert. Few-shot hash learning for image retrieval. In *Proceedings of the IEEE International Conference on Computer Vision Workshops*, pages 1228–1237, 2017.
- [28] Peter Welinder, Steve Branson, Takeshi Mita, Catherine Wah, Florian Schroff, Serge Belongie, and Pietro Perona. Caltech-ucsd birds 200. 2010.
- [29] Ronald J Williams. Simple statistical gradient-following algorithms for connectionist reinforcement learning. *Machine learning*, 8(3-4):229–256, 1992.
- [30] Shipeng Yan, Songyang Zhang, Xuming He, et al. A dual attention network with semantic embedding for few-shot learning. In *AAAI*, volume 33, pages 9079–9086, 2019.
- [31] Sangdoo Yun, Jongwon Choi, Youngjoon Yoo, Kimin Yun, and Jin Young Choi. Action-decision networks for visual tracking with deep reinforcement learning. In *Proceedings of the IEEE conference on computer vision and pattern recognition*, pages 2711–2720, 2017.